Persistent Heavy Rainfall over South China During May–August: Subseasonal Anomalies of Circulation and Sea Surface Temperature

HONG Wei (洪 伟) and REN Xuejuan* (任雪娟)

School of Atmospheric Sciences, Nanjing University, Nanjing 210093

(Received June 17, 2013; in final form August 23, 2013)

ABSTRACT

This study investigates the relationship between subseasonal variations of the circulation and sea surface temperature (SST) over the South China–East Asian coastal region (EACR) in association with the persistent heavy rainfall (PHR) events over South China during May–August through statistical analysis. Based on the intensity threshold and duration criterion of the daily rainfall, a total of 63 May–June (MJ) and 59 July–August (JA) PHR events are selected over South China from 1979 to 2011. The lower-level circulation anomalies on subseasonal timescale exhibit an anomalous cyclone over South China and an anomalous anticyclone shaped like a tongue over the South China Sea (SCS) during the PHR events for MJ group. The anomalous cyclone over South China in MJ originates from low-value systems in the mid-high latitudes before the rainfall. The anomalous anticyclone over the SCS is due to the westward extension of the western Pacific subtropical high (WPSH) and the southeastward propagation of the anomalous anticyclone from South China before the rainfall. For JA group, the lower-level anomalous circulation pattern is similar to that for MJ over the South China–EACR, but with different features of propagation. The subseasonal anomalous anticyclone is also related to the westward stretch of the WPSH, while the anomalous cyclone is traced back to the weak anomalous cyclone over the Philippine Sea several days before the rainfall events.

Positive SST anomaly (SSTA) is observed over the SCS and the Philippine Sea during the MJ PHR events on the subseasonal timescale. It is closely linked with the variation of local anomalous anticyclone. In contrast, negative SSTA occupies the South China coastal region for the JA PHR events, and it is driven by the anomalous cyclone which propagates northwestward from the Philippine Sea. The subseasonal positive (negative) SSTAs are generated via the local processes of above (below)-normal incident solar radiation and below (above)-normal latent heat fluxes. The possible role of the subseasonal SSTA in the local convective instability is also analyzed in this study.

Key words: persistent heavy rainfall, western Pacific subtropical high, subseasonal variations of sea surface temperature, South China

Citation: Hong Wei and Ren Xuejuan, 2013: Persistent heavy rainfall over South China during May–August: Subseasonal anomalies of circulation and sea surface temperature. *Acta Meteor. Sinica*, **27**(6), 769–787, doi: 10.1007/s13351-013-0607-8.

1. Introduction

The persistent heavy rainfall (PHR) is one kind of extreme meteorological disasters, which has attracted intensive research in China. There have been a lot of case studies on the PHR events. For example, Ding et al. (1993) analyzed the PHR over the Yangtze-Huai River basin (hereafter Jianghuai) during the summer of 1991. Jiang et al. (2011) investigated the PHR over the Huaihe River basin in 2007 on the perspective of water vapor transport and budget. Ding et al. (2010) studied the double rainbands in the PHR event over South China during June 2005. Niu et al. (2012) compared the circulation patterns during two PHR events to the south of the Yangtze River basin in the summer of 2010. On the climatological aspect, the PHR events in China during the last 50 years occur mostly over eastern China and South China (Bao, 2007; Chen and Zhai, 2013). The PHR events are distinguished from other types of extreme rainfall events with high

Supported by the National (Key) Basic Research and Development (973) Program of China (2012CB417203) and China Meteorological Administration Special Public Welfare Research Fund (GYHY201106017).

*Corresponding author: renxuej@nju.edu.cn.

intensity, broad extent, and long duration (Tang et al., 2006; Chen and Zhai, 2013).

Previous studies revealed that the PHR has a close relationship with the low-frequency oscillation (Lu and Ding, 1997; Shi and Ding, 2000; Yang et al., 2010; Cao et al., 2012, 2013). Lu and Ding (1997) suggested that low-frequency warm and moist air meets low-frequency cold air from north over the Jianghuai region, leading to three episodes of excessively heavy rainfall there during the summer of 1991. Shi and Ding (2000) demonstrated that the PHR during the summer of 1994 is closely related to the 30–60-day low-frequency propagation of the summer monsoon. Yang et al. (2010) identified two major modes of low-frequency oscillations (quasi-biweekly and 21–30-day) for the summer rainfall over the mid-lower reaches of the Yangtze River. Cao et al. (2012) suggested that the summertime PHR events over Southeast China occupy the active phase of the rainfall oscillation and exhibit significant quasi-biweekly features. They also demonstrated that the westward propagation of lower-level low-frequency signals from the South China Sea (SCS) and the Philippine Sea has important impacts on the PHR over Southeast China.

As a crucial component of the East Asian summer monsoon system, the western Pacific subtropical high (WPSH) has significant impacts on rainfall in China (Tao and Chen, 1987; Lu and Dong, 2001; Li and Zhu, 2010). Various studies revealed that the WPSH has a zonal oscillation on the subseasonal timescale, which corresponds to different stages of the PHR events (Mao and Wu, 2005; Tang et al., 2006; Bao, 2007; Wang et al., 2007; Ren et al., 2013). Mao and Wu (2005) suggested that an anomalous anticyclone and a cyclone exist alternatively over the coast of South China in the mode of a 15–35-day oscillation, modulating the WPSH extending westward or retreating eastward. Wang et al. (2009) demonstrated that the position of the WPSH is abnormally westward during the PHR events over South China, compared with its climatological state.

The circulation systems at upper levels are also important to the PHR occurrences. The South Asian high (SAH) has been shown to play an important role in causing the PHR over South China (Qian et al., 2002; Wang et al., 2007). Wang et al. (2007) suggested that the SAH moves westward during the PHR over South China in June 2005, which is in favor of triggering the PHR. The cooperation of upper-level circulation and lower-level circulation is vital in the PHR events. Cao et al. (2012) demonstrated that there are two upper-level low-frequency signals affecting the summertime PHR in Southeast China: southeastward propagation from the area 30°–45°N, 50°–70°E and westward propagation from the Philippine Sea. These signals are favorable for the anomalous divergence circumstance over Southeast China during the PHR events at upper levels.

The sea surface temperature anomaly (SSTA) can exert significant impacts on circulation and rainfall on multiple timescales (Huang and Wu, 1989; Lu and Dong, 2001; Chan and Zhou, 2005; Lau and Nath, 2009; Zhou et al., 2009). Recently, the subseasonal SST variability has attracted more and more attention with the advent of new satellite-based estimates of SST (Vecchi and Harrison, 2002; Wu et al., 2008; Wu, 2010; Wang and Zhou, 2012; Ren et al., 2013). Vecchi and Harrison (2002) showed that there exists subseasonal SST variability over the Indian monsoon region, and the cooling of SST in the Bay of Bengal precedes monsoon breaks by about a week. Wu et al. (2008) demonstrated that SST over the summer monsoon region including the SCS has notable subseasonal fluctuations. Their investigation also indicated that the convection-SST interaction on the subseasonal timescale is most notable in the summer hemisphere. Yin et al. (2011) demonstrated that the SSTA over the Kuroshio and its extension region can influence the intensity of Meiyu quasi-biweekly oscillation by air-sea interaction. The possible mechanisms in the subseasonal air-sea interaction are also analyzed in some studies. The mechanisms include wind-evaporation and cloud-radiation processes. Meanwhile, the variation of SST can modulate circulation via changing the lower-level convective instability (Roxy and Tanimoto, 2012; Wang et al., 2012; Ren et al., 2013).

Many previous studies focused on case studies of the PHR events and associated low-frequency atmospheric circulation. Few studies have analyzed the PHR events over South China and related subseasonal

circulation during May–August on climatological aspect. Furthermore, subseasonal SST variability over the East Asian coastal region (EACR) during the PHR events is not clear yet. In this study, we investigate the features of the circulation and SSTA over South China–EACR during the PHR events in May–August on the subseasonal timescale. Previous work showed that the subseasonal mean states regulate the 12–20-day oscillation over eastern China (Yang et al., 2013). The circulation pattern for PHR events over South China in May–June (MJ) has great differences from that in July–August (JA) (Bao, 2007; Hu et al., 2007; Qiang and Yang, 2008; Wang and Ding, 2008; Wang et al., 2009). The PHR over South China in MJ is mostly influenced by the summer monsoon system while the PHR in JA is strongly related to the typhoon and the movement of the intertropical convergence zone (ITCZ) (Ding and Chan, 2005). Thus, in this study, we analyze the PHR events over South China by two groups: the MJ and JA PHR events.

The structure of the article is as follows. Section 2 gives a brief description of data and method. Section 3 analyzes evolution of the subseasonal atmospheric circulation accompanied with two groups of PHR events over South China. Section 4 investigates the features and evolution of subseasonal SSTA during the PHR. Section 5 provides the conclusion and discussion.

2. Data and method

2.1 Data

In this study, we use the daily rainfall dataset at 756 gauge stations in the period of 1979–2011 from the China Meteorological Administration (CMA) to identify the PHR events. We use the National Centers for Environmental Prediction-Department of Energy (NCEP-DOE) Atmospheric Model Intercomparison Project-II (AMIP-II) reanalysis daily data (Kanamitsu et al., 2002) to analyze the features of circulation and heat fluxes. The daily outgoing longwave radiation (OLR) with a spatial resolution of 2.5°×2.5° from the National Oceanic and Atmospheric Administration (NOAA) is also adopted to investigate the activities of convection (Liebmann and Smith, 1996). The above referred variables are all from 1979 to 2011. The SST dataset is from Version 2 of the NOAA Optimal Interpolation with a spatial resolution of 0.25°×0.25° and temporal resolution of 1 day from 1982 to 2011.

2.2 Method

A single-station PHR event is defined when the station rainfall intensity is $\geqslant$ 25 mm day^{-1} and duration lasts for not less than 3 days. Figure 1 shows the distribution of total number of single-station PHR events and corresponding averaged rainfall intensity over mainland China during MJ and JA 1979–2011. Figure 1a shows that PHR events occur most frequently to the south of the Yangtze River basin for the MJ group, and the strongest rainfall intensity also occurs in this region (Fig. 1c). For the JA group, most PHR events occur south of 25°N (Fig. 1b). There are two regions with larger rainfall intensity: South China and Jianghuai (Fig. 1d). In conclusion, both frequency and intensity of the single-station PHR over South China are prominent. Therefore, we choose South China (20°–25°N, 105°–120°E) as our research area. In this region, we select 47 gauge stations for choosing the PHR events (red dots in Fig. 1a).

In order to identify the dominant periodicity, the power spectrum analysis is applied to the averaged 47 stations' daily rainfall time series over South China during each May–August from 1979 to 2011. Before applying the power spectrum analysis, we first removed the seasonal cycle from the rainfall dataset, and then eliminated the high frequency oscillation by applying an 8-day running mean. Figure 2 shows the 1979–2011 averaged results of the power spectrum analysis over South China. We can see that 12–30-day period is statistically significant, suggesting that the rainfall during May–August over South China has notable subseasonal oscillations. In order to isolate the subseasonal signals, we apply the 12–30-day bandpass filter to all the variables in this study.

The above daily rainfall time series over South China, which have been applied with 12–30-day bandpass filter, are normalized to unit standard deviation. The final time series are named as the subseasonal rainfall anomaly index (RI). We use the RI to identify the PHR events over South China. If the RI exceeds

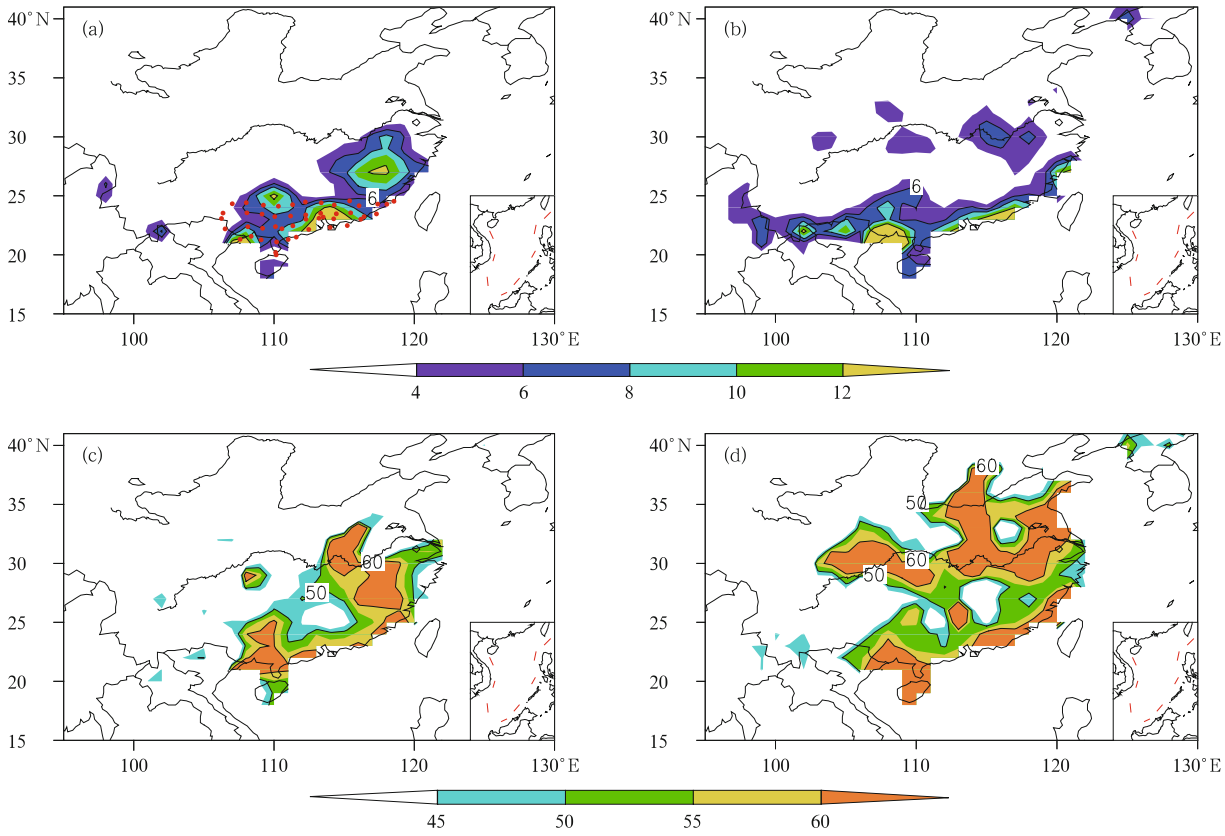

Fig. 1. Total number of single-station PHR events during (a) May–June and (b) July–August of 1979–2011 (shaded) with criteria of intensity $\geqslant$ 25 mm day^{-1} and duration $\geqslant$ 3 days, and the average intensity (mm day^{-1}) of single-station PHR events during (c) May–June and (d) July–August of 1979–2011 (shaded). The red dots in (a) show the location of the 47 raingauge stations used in this study.

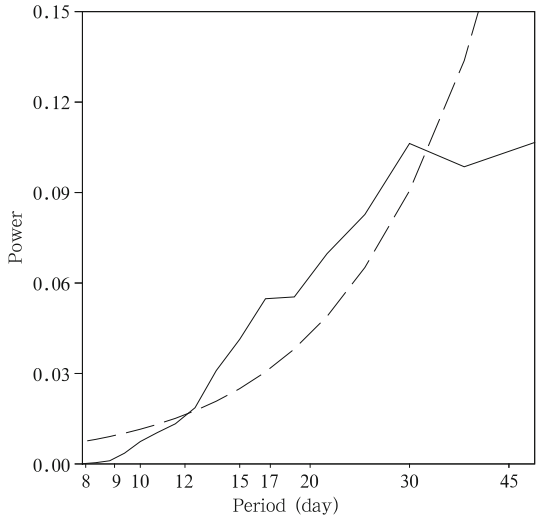

Fig. 2. Power spectrum analysis of the rainfall over South China during May–August of 1979–2011. The dashed line is for the red noise spectrum.

one standard deviation for at least three successive days, we define it as one PHR event for South China. Figure 3 shows examples of the daily rainfall and RI time series during May–August of 1994 and 2005. By using this method, we obtain 63 PHR events for MJ and 59 PHR events for JA. For most PHR events, the duration ranges from 3 to 7 days. Based on these PHR events, the leading-lag composite is used in the following analysis to examine evolution of the atmospheric circulation and SSTA signals on the subseasonal timescale. The simultaneous composite is applied by averaging the variables for all the days that are included in the PHR events from 1979 to 2011. The leading (lag) composite is obtained by shifting forward (backward) the number of leading (lag) days.

We also calculate the total column water vapor (W) and water vapor flux (F_x, F_y) in this study, and

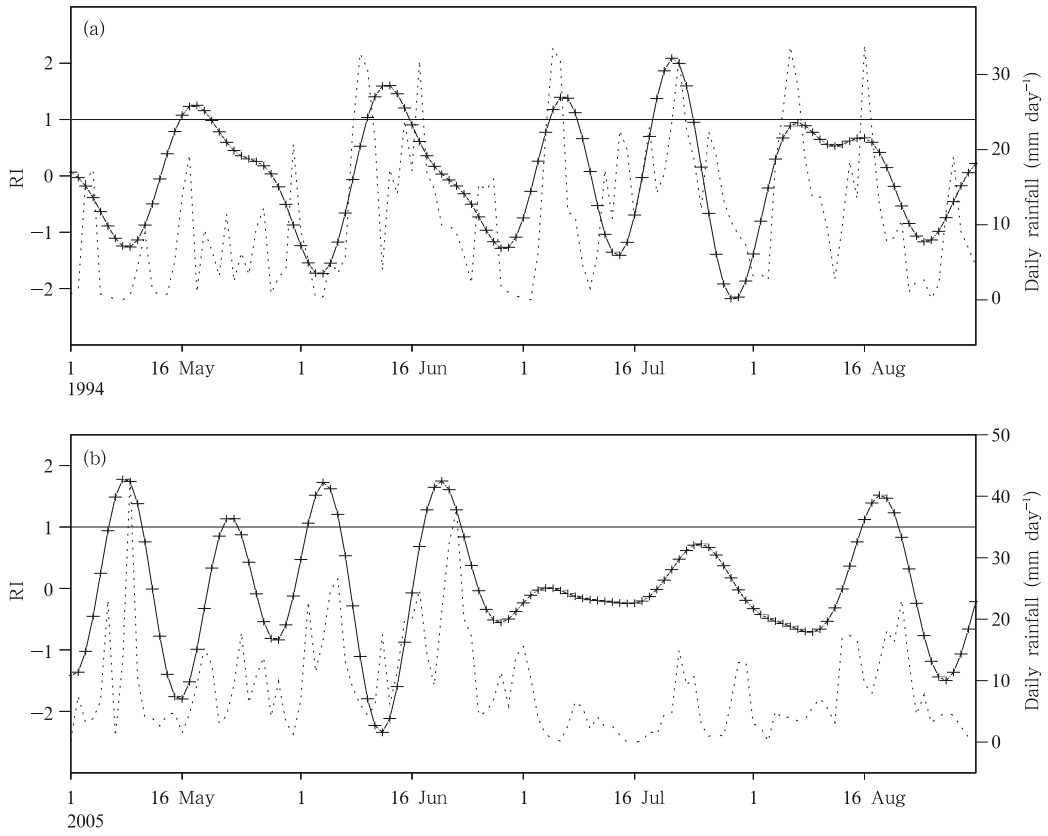

Fig. 3. Time series of the daily rainfall (dot line; mm day^{-1}) and subseasonal rainfall anomaly index (RI; solid with plus marks) averaged over South China for the cases of (a) 1994 and (b) 2005, respectively.

they are defined as follows:

$$W = \frac{1}{g}\int_{p_t}^{p_s} q\mathrm{d}p,$$

$$F_x = \frac{1}{g}\int_{p_t}^{p_s} qu\mathrm{d}p,$$

$$F_y = \frac{1}{g}\int_{p_t}^{p_s} qv\mathrm{d}p,$$

p_s means surface air pressure (we use 1000 hPa here), p_t uses the air pressure at 500 hPa due to the fact that water vapor resides mostly at mid-lower levels, g is the acceleration of gravity, u, v, and q are zonal and meridional winds, and specific humidity, respectively.

3. Subseasonal circulation features

Figures 4a and 4c show the simultaneous composite of subseasonal 850-hPa geopotential height (Z850) anomaly and 850-hPa wind field anomaly superimposed on 5880–5860-gpm contour lines for MJ and JA groups. During MJ (Fig. 4a), an anomalous cyclone is located over South China while an anomalous anticyclone lies over the EACR accompanied with PHR events. The southwest side of the anomalous anticyclone shaped like a tongue occupies the SCS. This anomalous pattern is in favor of convergence of water vapor over South China, leading to the PHR events there. Meanwhile, the west point of the WPSH represented by the 5880-gpm contour line (5880-line) is located at 120°E and extends to the tongue area of the anomalous anticyclone (hereafter tongue area). This means that the tongue area may have a close relationship with the changes of the WPSH. The circulation pattern in JA has some similarities with that in MJ, whereas the tongue area over the SCS has a stronger intensity and broader extent (Fig. 4c). Besides, there is a center of positive Z850 anomaly over 20°–30°N,

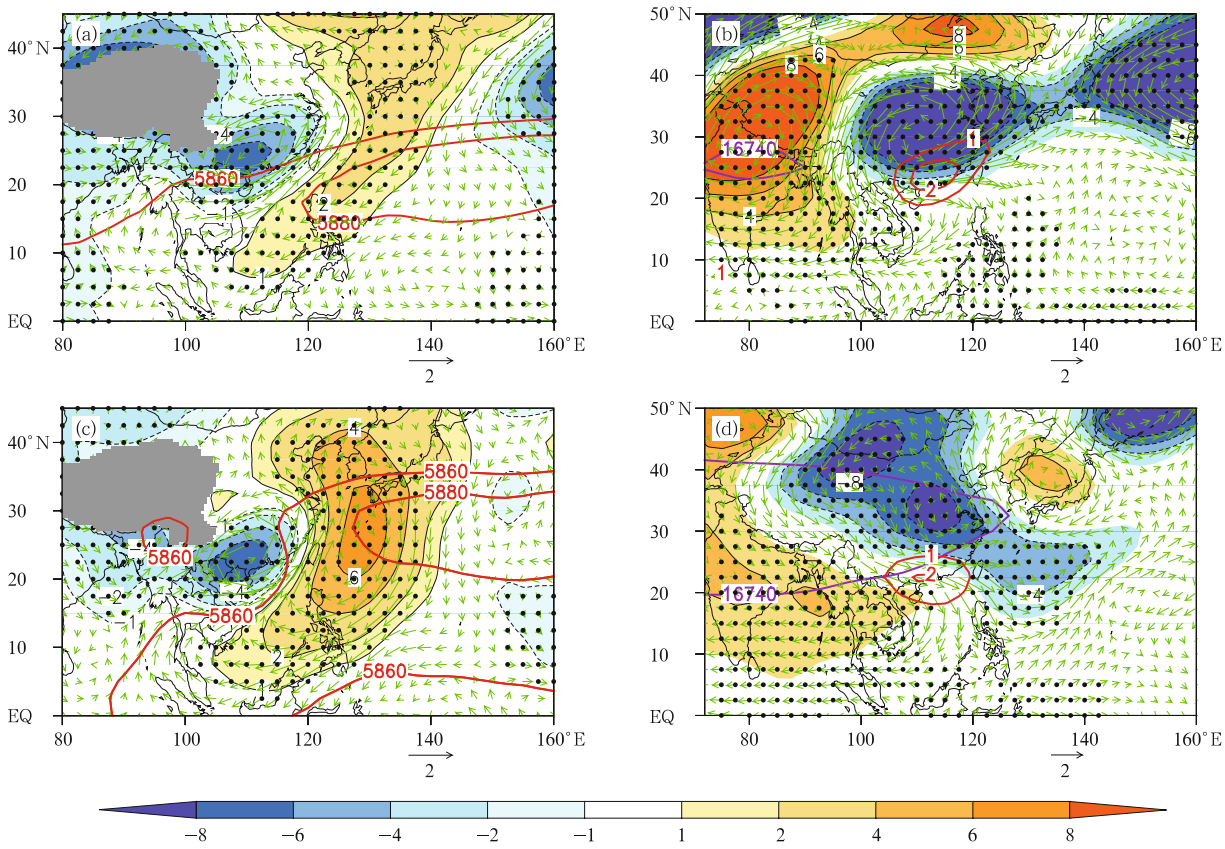

Fig. 4. Simultaneous composite of subseasonal wind anomaly at 850 hPa (vector; m s^{-1}) and Z850 anomaly (shaded and black contour; gpm) for (a) 63 MJ PHR events and (c) 59 JA PHR events. Panels (b) and (d) are the same as (a) and (c), but for the wind anomaly at 200 hPa and Z200 anomaly. Composites of 5880-line at 500 hPa (red contour; a, c) and 16740-line at 100 hPa (purple contour; b, d) for MJ and JA groups are also shown. The red contour lines in (b) and (d) show the divergence of 200-hPa wind anomaly. The black dots in (a–d) denote the areas with above the 95% *t*-test confidence level for Z850 and Z200 anomaly.

125°–135°E, which does not exist in MJ. Compared with the pattern in MJ, the WPSH in JA, with its west point located at the center of positive Z850 anomaly, moves northward and occupies a larger area. The convergence in JA is still dominant like that in MJ, which is conducive to excessive rainfall over South China in JA. Above analysis shows that the WPSH changes, and the anomalous cyclone and anticyclone over South China–EACR are important for the PHR events. Their evolution during the PHR events will be investigated later in Figs. 5–7.

Figures 4b and 4d plot simultaneous composite of subseasonal 200-hPa geopotential height (Z200) anomaly and 200-hPa wind field anomaly for two groups of PHR events. We use 16740-gpm contour line (16740-line) at 100 hPa to represent the intensity and extent of the SAH for the two groups. For MJ group (Fig. 4b), the east point of 16740-line lies at 90°E. The subseasonal Z200 anomaly exhibits an east-west dipole structure with the west lobe located mainly over 20°–40°N, 70°–90°E and the east one over southeastern China. Both the negative and positive lobes are above the 95% confidence level. The distribution of wind anomaly at 200 hPa shows that the westerly anomaly along the 20°N-latitude line over South China splits up into two branches with one branch going northeastward and the other going southeastward. This feature forms an anomalous divergence condition at the upper levels over South China.

For JA group (Fig. 4d), the east point of 16740-line reaches 128°E during the PHR events. The subseasonal Z200 anomaly exhibits a northeast-southwest

dipole structure with smaller amplitude compared with that in MJ. The northeast (negative) lobe covers mainland China, and the southwest (positive) one covers the area from India to Indochina Peninsula. We notice that the strong anomalous divergence occurring over South China in JA is similar to the condition in MJ. Overall, for both groups (MJ and JA), there exist anomalous divergence at the upper levels and anomalous convergence at the lower levels over South China in accompanion with the PHR.

The above analysis of simultaneous fields in Figs. 4a and 4c demonstrates that lower-level patterns of anomalous cyclone over South China and anomalous anticyclone over the EACR are dominant for both MJ and JA PHRs. The tongue area over the SCS may be closely related to the WPSH variation. In the following, we examine the evolution of the WPSH during the PHR events.

Figure 5 displays the evolution of 5880-line from lag = –8 to lag = 8 with an interval of 2 day for the two groups. The negative (positive) lag indicates a leading (lagging) situation prior to (post) the PHR events. For MJ group (Figs. 5a and 5c), the west point of the WPSH is located at about 125°E at lag = –8. Then, it extends westward to about 121°E at lag = –6. The WPSH stays nearly motionless at 120°E from lag = –6 to lag = –2 before the WPSH reaches the westernmost point at lag = 0 (119°E). From lag = 0 to lag = 4, the WPSH withdraws northeastward with smaller amplitude. For JA group (Figs. 5b and 5d), the main body of the WPSH is located more northeastward in general compared with that in MJ. At lag = –8, the west point of the WPSH is located at 133°E. Then, it stretches westward continuously and slowly before reaching the westernmost point at lag = 0 (128°E). After the rainfall event, the WPSH retreats eastward to 135°E step by step from lag = 0 to lag = 8. The mean state of the WPSH in MJ is also very different from that in JA (Figs. 5a and 5b) because of the northward migration of the WPSH during the boreal summer. Previous

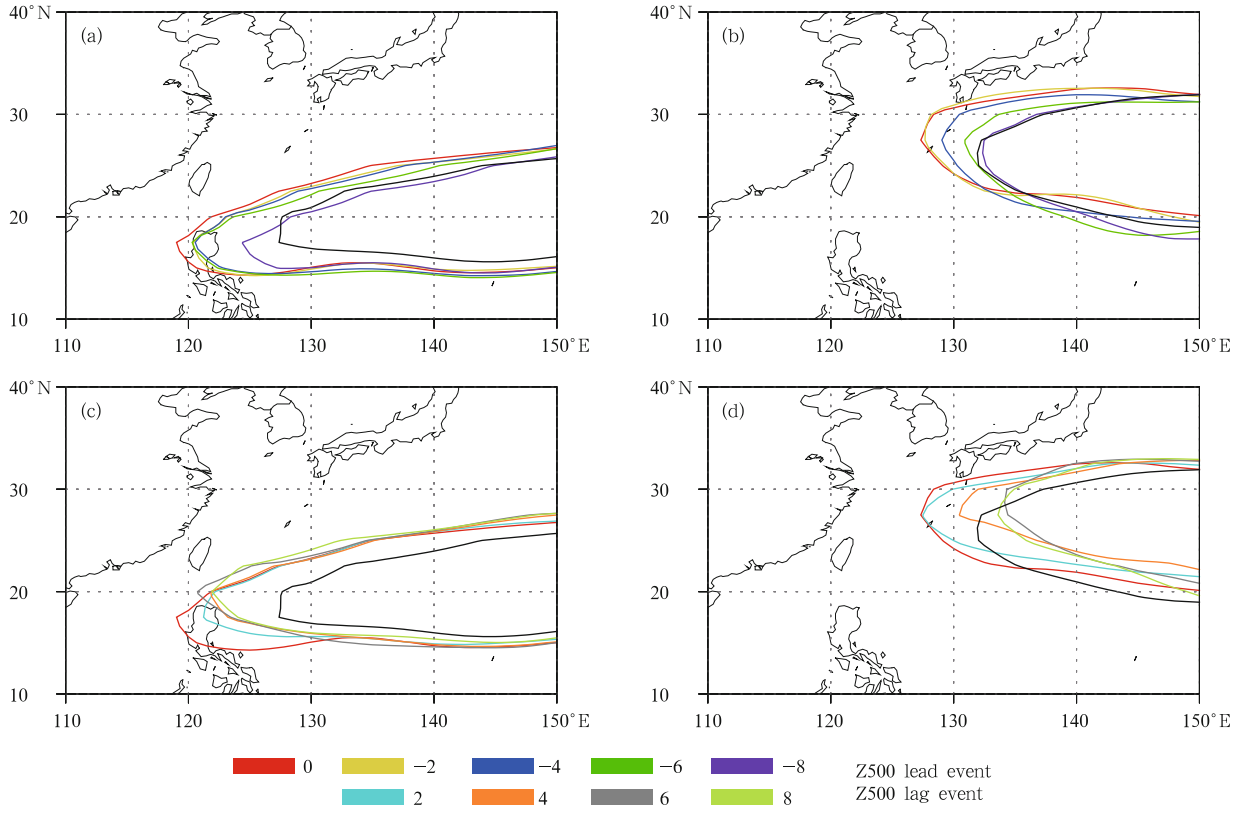

Fig. 5. Lagged composite of 5880-gpm lines for (a, c) MJ and (b, d) JA events: (a, b) for Z500-field lead events and (c, d) for Z500-field lag events from 8 to 0 days with an interval of 2 days, respectively. The black contours represent the mean state of the 5880-line averaged from 1979 to 2011.

studies have shown that the subseasonal march of the summer monsoon circulation has effects on the change in behavior of 12–20-day oscillations over eastern China (Yang et al., 2013). We thereby infer that the change of the mean state of the WPSH between MJ and JA may be an important reason for the subseasonal circulation differences around the tongue area between the two groups of PHR shown in Figs. 4a and 4c.

The evolution of the WPSH at 500 hPa for the two groups exhibits similar characteristics: the WPSH stretches westward before the rainfall, gets its westernmost point during rainfall events, and then withdraws eastward after the rainfall events. Thus, the westward stretch of the WPSH may partially lead to the formation of the anomalous anticyclone over the EACR, especially the formation of the tongue area over the SCS. To clarify the speculation, Fig. 6 depicts the evolution of the characteristic geopotential contour lines at 850 hPa which represent the lower-level WPSH for the two groups. The 1505-line is used for the MJ group (Figs. 6a and 6c) while the 1490-line is used for the JA group (Figs. 6b and 6d). For MJ group, the intersection point between the 1505-line and the 10°N-latitude line is used to depict the zonal movement of the lower-level WPSH. The intersection point moves westward slowly from 122° to 118°E prior to the rainfall (from lag = –8 to lag = 0), and after the rainfall, it retreats eastward quickly and reaches 125°E at lag = 8. For JA group, we use the intersection point between the 1490-line and the 20°N-latitude line to display the zonal movement of the 850-hPa WPSH. The intersection point lies at 128°E at lag = –8 and stretches to 122°E at lag = 0. Then, it continuously extends westward from lag = 0 to lag = –2. After that, the WPSH retreats eastward with a large span of 8 degrees from lag = 2 to lag = 6. When the WPSH is located at the westernmost point, the anomalous anticyclone shaped like a tongue also occupies the SCS. Therefore, the westward stretch of the WPSH has a close linkage with the tongue area.

In order to examine the prior signals of the subseasonal anomalous cyclone and anticyclone over the

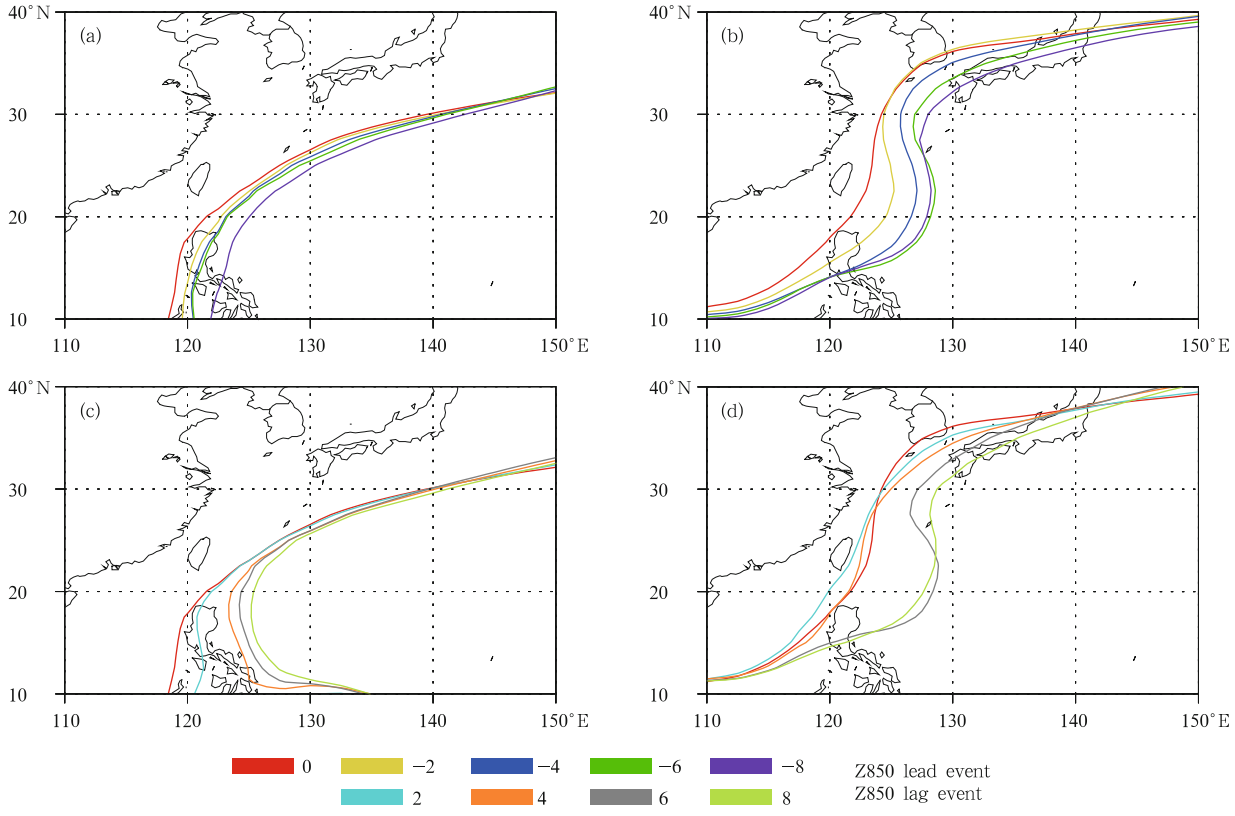

Fig. 6. As in Fig. 5, but for the evolution of the (a, c) 1505-line and (b, d) 1490-line at 850 hPa.

South China–EACR, Fig. 7 shows the Hovmöller plots of subseasonal 850-hPa relative vorticity (ζ_{850}) anomaly for two groups of PHR events averaged over 10°–25°N, 105°–120°E, from lag = –15 to lag = 15. For MJ group (Fig. 7a), the positive anomaly (anomalous cyclone) occurs at about 45°N around lag = –10, and it propagates continuously southward and reaches 32°N around lag = –7. Then, the positive ζ_{850} anomaly continues moving southward and reaches South China with its largest amplitude at the beginning of the PHR events. Therefore, in MJ, the southward propagation of the positive ζ_{850} anomaly from mid-high latitude is an important precursor signal for the PHR events over South China. Several studies about the heavy rainfall during the pre-rainy season over South China also demonstrated similar signals (Wu et al., 2006; Pan et al., 2013). For instance, Wu et al. (2006) suggested that the first flood period over South China is closely related to southward propagation of the low value system at its north side. Figure 7a also shows that the southward propagation of negative ζ_{850} anomaly (anomalous anticyclone) from South China (25°N) to the SCS (15°N) during lag = –10 to lag = 0 period is a potential contributor to the formation of the tongue area. Figure 7c shows that there are two precursor signals for the tongue area on the aspect of zonal propagation. One signal is the eastward propagation of negative ζ_{850} anomaly from 105° to 120°E during lag = –10 to lag = 0 period, which is identical with the above southward propagation of negative ζ_{850} anomaly in Fig. 7a. The other signal is the westward propagation of the negative ζ_{850} anomaly from the Philippine Sea (140°E) to the SCS (120°E) during lag = –10 to lag = 0 period, which corresponds to the westward extension of the WPSH. Therefore, both the southeastward propagation of the anomalous anticyclone from South China and the westward stretch of the WPSH contribute to the formation of the tongue area in MJ as shown in Fig. 4a.

For JA group (Figs. 7b and 7d), the subseasonal

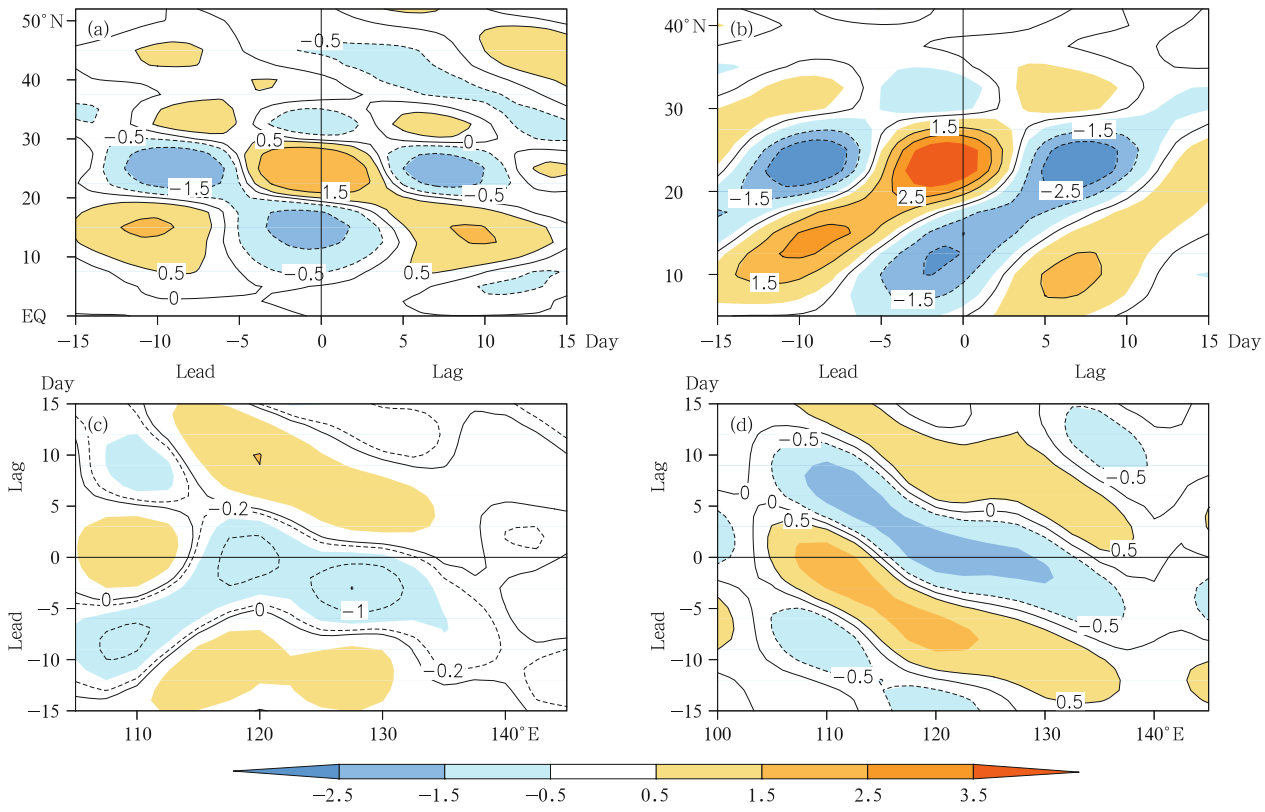

Fig. 7. Hovmöller plots of subseasonal anomalies of relative vorticity at 850 hPa for (a, c) MJ and (b, d) JA events over (a, b) 105°–120°E and (c, d) 10°–25°N. Negative (positive) lags on the (a, b) abscissa and (c, d) ordinate mean that relative vorticity anomalies lead (lag) rainfall. Lag = 0 corresponds to simultaneous composite.

anomalous cyclone exhibits different evolution. The positive ζ_{850} anomaly (anomalous cyclone) over South China during the PHR events is traced back to the weak positive ζ_{850} anomaly over the Philippine Sea (10°N, 135°E; at lag = –15). Prior to the rainfall, the weak positive ζ_{850} anomaly over the Philippine Sea propagates northwestward to South China and strengthens gradually. The westward propagation of the negative ζ_{850} anomaly from 140° to 120°E (from lag = –8 to lag = 0) in Fig. 7d indicates that the formation of the tongue area is closely related to the westward stretch of the WPSH.

Figure 8 displays the Hovmöller plots of subseasonal anomaly of relative vorticity at 200 hPa for MJ and JA groups. This is to exhibit the evolution of the anomalous cyclone over mainland China as shown in Figs. 4b and 4d. For MJ group, the positive 200-hPa relative vorticity (ζ_{200}) anomaly (anomalous cyclone) exhibits southward propagation from 45° to 30°N in Fig. 8a and eastward propagation from 60° to 110°E in Fig. 8c prior to the rainfall (from lag = –15 to lag = 0). This feature indicates that the mid-high latitude systems propagate southeastward and trigger the subseasonal anomalous cyclone over southeastern China. Pan et al. (2013) indicated the 10–20-day oscillation of the spring rainfall over South China appears to be a southeastward propagating coherent wave train comprising a series of anomalous cyclones and anticyclones, which is similar to our results. For JA group (Figs. 8b and 8d), the positive ζ_{200} anomaly (anomalous cyclone) also appears southward propagating from 60° to 30°N during lag = –8 to lag = 0, but the zonal propagation is not remarkable. The activities of cold air affecting South China in MJ are more active than that in JA (Liang and Wu, 2001; Bao, 2007). Therefore, the different mean states may be the reason for the different features of propagation between the two groups of PHR events shown in Figs. 7 and 8.

Figure 9 shows the Hovmöller plots of subseasonal

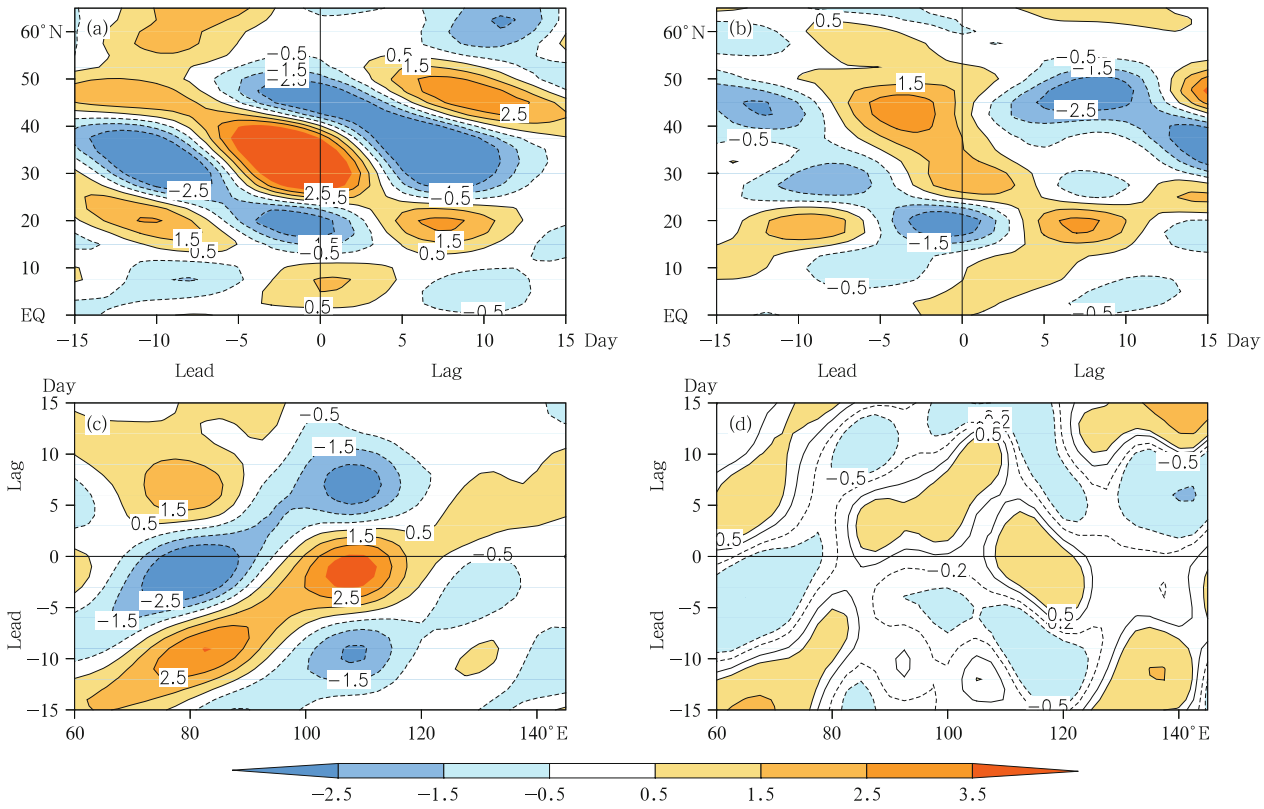

Fig. 8. Hovmöller plots of subseasonal anomalies of relative vorticity at 200 hPa for (a, c) MJ events and (b, d) JA events over (a, b) 100°–120°E and (c, d) 20°–40°N.

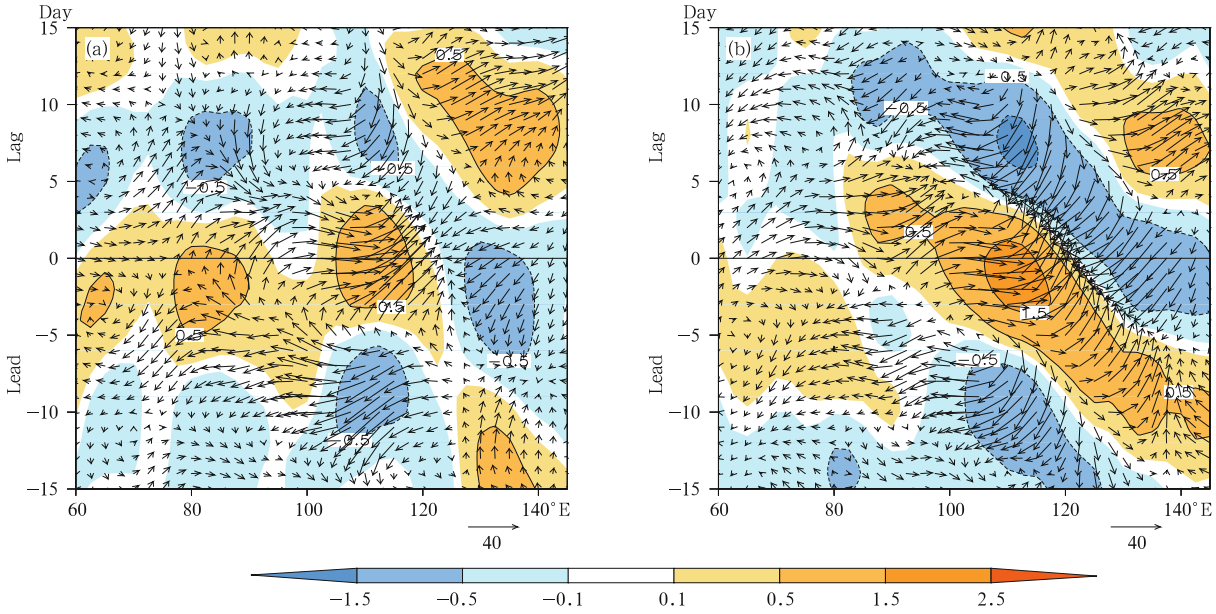

Fig. 9. Hovmöller plots of subseasonal anomalies of total column water vapor (shaded; kg m^{-2}) and water vapor flux (vector; kg m^{-1} s^{-1}) for (a) MJ and (b) JA events over 10°–25°N.

total column water vapor anomalies and water vapor flux anomalies for the two groups of PHR events averaged over 10°–25°N, from lag = –15 to 15. For MJ group (Fig. 9a), water vapor can be transported to South China from two paths. One is the eastward propagation from the Bay of Bengal (90°E) to South China (115°E) during lag = –5 to lag = 0. The other path is the westward propagation from the western Pacific (140°E) to South China (115°E) during lag = –15 to lag = 0. The westward transport of water vapor may be related to the westward stretch of the WPSH. For JA group (Fig. 9b), the positive total column water vapor anomaly propagates westward from 140° to 120°E from lag = –12 to lag = 0, accompanied with strong westward stretch of northeastward water vapor flux, which is closely related to the westward extension of the WPSH. Overall, the westward stretch of WPSH is in favor of the westward transport of water vapor.

4. Subseasonal features of SSTA

In this section, we investigate the features of SST variability over the EACR on the subseasonal timescale in association with the PHR events over South China. Figure 10 shows simultaneous composite of SSTA on the subseasonal timescale linked with two groups of PHR events. For MJ group (Fig. 10a), there is a large area of positive SSTA over the SCS and the Philippine Sea while a small area of negative SSTA appears along the East Asian coastal line. The positive SSTA lies beneath the WPSH and corresponds well to the tongue area. We define area 1 (5°–20°N, 112°–132°E) in Fig. 10a as the key oceanic region, in order to investigate the relationship between the positive SSTA and the evolution of the anomalous anticyclone. For JA group (Fig. 10b), robust negative SSTA occurs over the South China coastal region during the PHR events. Figures 7b and 7d show that the subseasonal anomalous cyclone propagates northwestward from the Philippine Sea and passes by the South China coastal region just before the PHR events. The negative SSTA over the South China coastal region may have been related to the anomalous cyclone. Thus, we define area 2 (14°–24°N, 108°–124°E) in Fig. 10b as the key region for JA group. In the following, the co-variation of SSTA and circulation anomaly on the subseasonal timescale is investigated over the above defined two areas (area 1 and area 2).

4.1 Subseasonal co-variation of SSTA and 850-hPa circulation anomalies

To examine the co-variation of the SSTA and cir-

culation anomaly on the subseasonal timescale, the Hovmöller plots of subseasonal anomalies of SST and Z850 for MJ group over area 1 are shown in Figs. 11a and 11c. The positive Z850 anomaly (anomalous anticyclone) occurs first around lag = –8 over 5°–20°N (Fig. 11a) and 112°–132°E (Fig. 11c). The amplitude of the positive Z850 anomaly begins to increase and reaches the maximum at about lag = –3, which is related to the southeastward propagation of the anomalous anticyclone from South China and the westward extension of the WPSH mentioned above. Then, the positive Z850 anomaly weakens and switches to negative Z850 anomaly from lag = –3 to lag = 12. On the oceanic aspect, the notable negative SSTA over area 1 occurs at lag = –9, 3 days after the prominent negative Z850 anomaly at lag = –12. Then, the negative SSTA fades and switches to positive SSTA from lag = –9 to lag = 1. The prominent positive SSTA occurs at about lag = 1, which is 4 days delayed after the prominent positive Z850 anomaly over area 1. This feature indicates a phase difference between the subseasonal anomalies of SST and circulation. For MJ group, the subseasonal SSTA over area 1 lags 3 or 4 days behind the Z850 anomaly.

Figures 11b and 11d show the Hovmöller plots of subseasonal anomalies of SST and Z850 for JA group over area 2. For JA group, we investigate the variation of SSTA and anomalous circulation over area 2. Figure 11b shows that the negative Z850 anomaly over 14°–24°N reaches its largest amplitude around lag = –3, which is linked with the above northwestward propagation of the anomalous cyclone from the Philippine Sea. Afterward, it weakens and switches to positive Z850 anomaly in several days. Figure 11d shows the same feature over the area of 108°–124°E. During the PHR events, the maximum amplitude of the negative SSTA appears over area 2 at lag = 1, about 4 days behind the maximum amplitude of the negative Z850 anomaly at lag = –3. Therefore, the subseasonal SSTA lags about 4 days behind the Z850 anomaly for JA group.

4.2 Causes of the subseasonal SSTAs

To further investigate the phase difference between the subseasonal SSTA and circulation anomaly and the causes of the subseasonal SSTAs, Figs. 12a and 12b display co-variation of subseasonal Z850 anomaly and SSTA averaged over area 1 and area 2. For area 1 during MJ, the subseasonal Z850 leads SSTA by about 4 days (Fig. 12a). For area 2 during JA, the subseasonal Z850 anomaly also leads SSTA by 4 days (Fig. 12b). The results present the phase

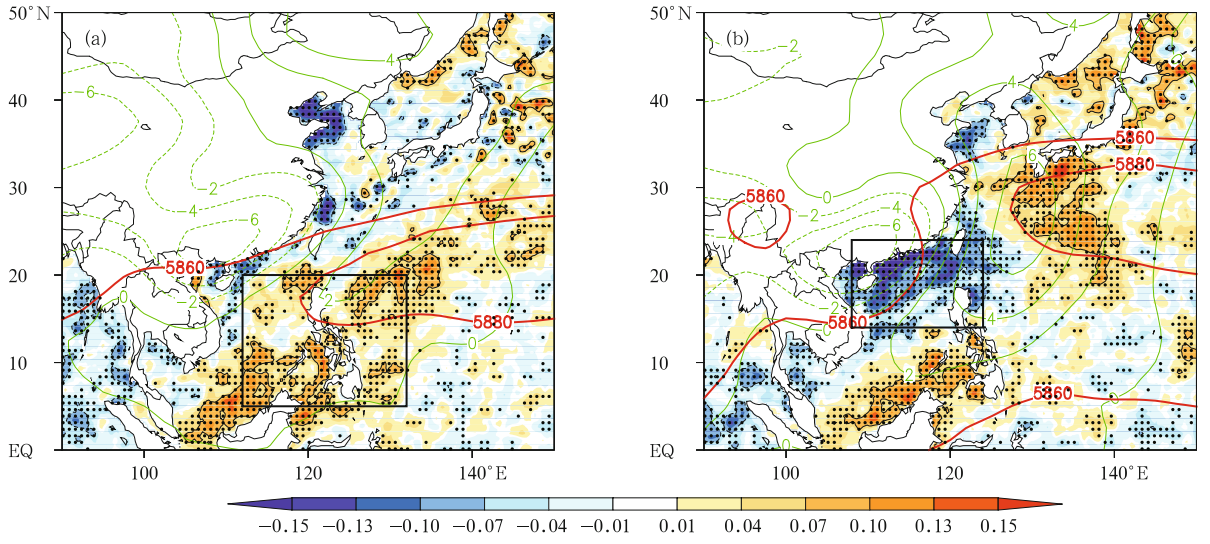

Fig. 10. Simultaneous composite of subseasonal SSTA (shaded; K) for (a) MJ and (b) JA PHR events. Composites of 5880–5860-gpm contour lines (red contours) and Z850 anomaly (green contours; gpm) are overlapped. The black dots denote the areas above the 95% t-test confidence level for the subseasonal SSTA. The box in (a) denotes area 1 (5°–20°N, 112°–132°E) and the box in (b) area 2 (14°–24°N, 108°–124°E).

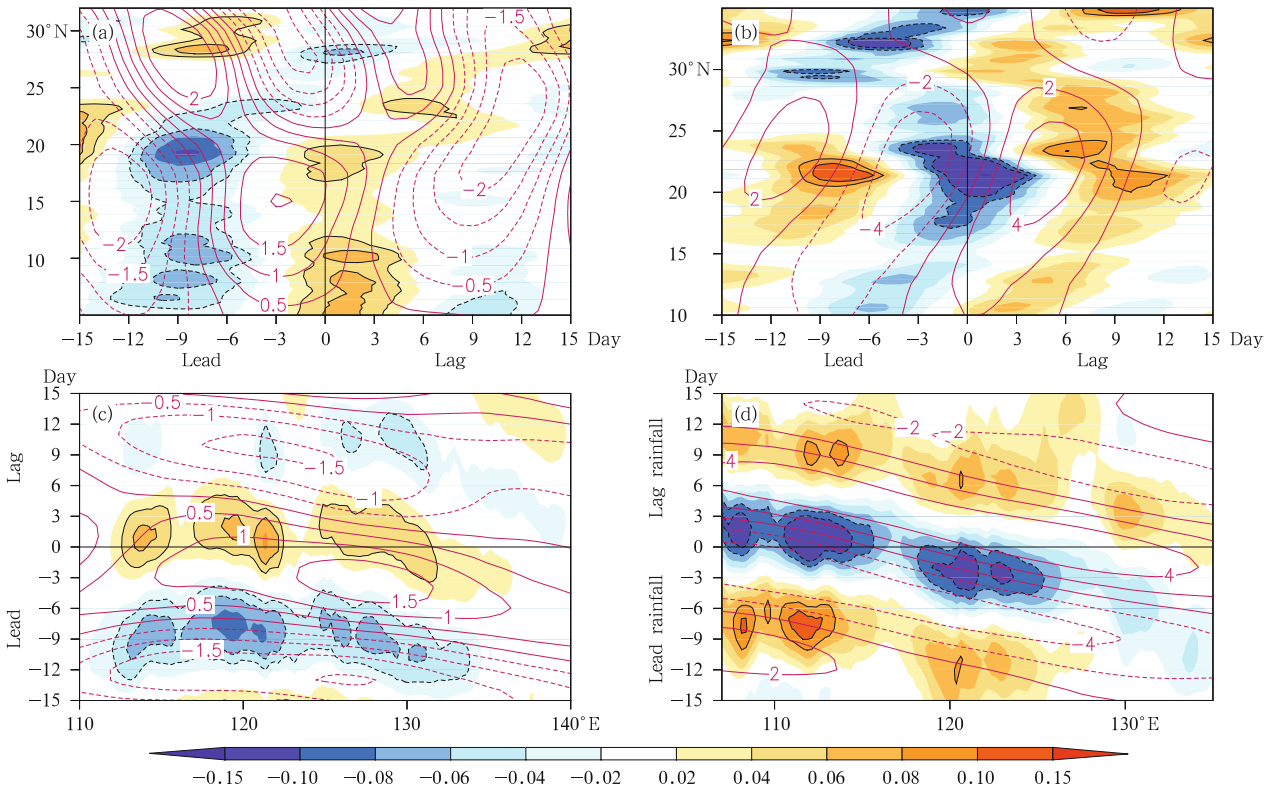

Fig. 11. Hovmöller plots of subseasonal anomalies of SST (shaded; K) and Z850 (red contour; gpm) for MJ events over (a) 112°–132°E and (c) 5°–20°N corresponding to area 1 in Fig. 10a. Panels (b) and (d) are the same as (a) and (c), but for JA events over (b) 108°–124°E and (d) 14°–24°N (area 2). Negative (positive) lags (day) on the abscissa mean that SST (Z850) anomalies lead (lag) rainfall. Lag = 0 corresponds to simultaneous composite.

difference more clearly. Therefore, for MJ group, the positive SSTA over area 1 is closely related to the variation of local anomalous anticyclone. For JA group, the negative SSTA over area 2 has a close relationship with the northwestward propagation of the anomalous cyclone from the Philippine Sea.

How does the subseasonal circulation anomaly affect the subseasonal SSTA? There are two major ways: one is via the radiation and heat fluxes, and the other is via upper ocean physical processes. Previous studies have demonstrated that the former is more important on subseasonal timescales (Wu, 2010; Roxy and Tanimoto, 2012). We try to explain causes of the subseasonal SSTA on the perspective of radiation and heat fluxes. Figure 12 also shows the composite of subseasonal anomalies of OLR and net solar and net longwave radiations, latent and sensible heat fluxes, wind speed at 10 m, and specific humidity at 2 m, which are all averaged over area 1 and area 2. For area 1 during MJ (Fig. 12c), the net solar radiation anomaly changes from minimum to maximum from lag = –9 to lag = 0. The OLR anomaly are enhanced from lag = –12 to lag = –2 and suppressed from lag = –2 to lag = 8. The variation of OLR and net solar radiation anomaly corresponds well to the westward extension of the WPSH and the southeastward propagation of the anomalous anticyclone from South China. The convection is not active and there is little cloud over area 1 during this process, thus in favor of the increase of SSTA. The net longwave radiation anomaly is relatively small compared with the net solar radiation anomaly. Figure 12e shows that the subseasonal latent heat anomaly varies from the positive maximum (lag = –11) to the negative maximum (lag = –1). This is mainly because of the decrease of the surface wind anomaly (Fig. 12g). This feature shows that the ocean over area 1 releases less energy to the atmosphere, which is also in favor of the in-

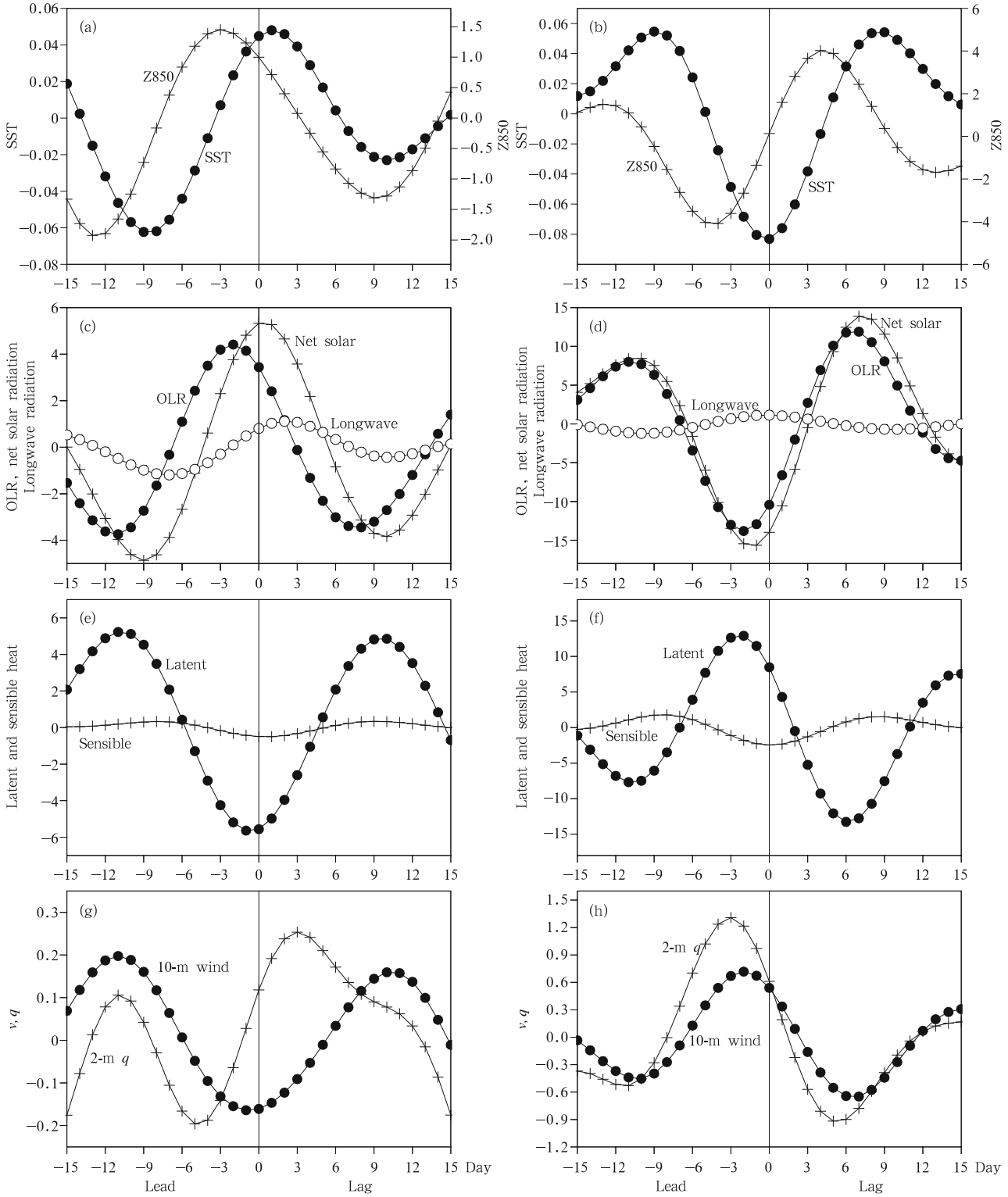

Fig. 12. (a, b) Composite subseasonal anomalies of SST (dot line; K) and Z850 (cross line; gpm); (c, d) OLR (dot line), net solar radiation (cross line), and net longwave radiation (hollow dot line) (W m^{-2}); (e, f) latent (dot line) and sensible heat (cross line) fluxes (W m^{-2}), and (g, h) wind speed at 10 m (dot line; m s^{-1}) and specific humidity at 2 m (cross line; 10^{-4} kg kg^{-1}), averaged over (a, c, e, g) area 1 and (b, d, f, h) area 2.

crease of SSTA there. The amplitude of the sensible heat anomaly is so small that it is neglected.

Overall, before the rainfall, the occupation of the anomalous anticyclone over area 1 triggers more radiation and less cloud there, so the ocean over area 1 receives more radiation and releases less latent heat to the atmosphere, which is favorable for the increase of SSTA. After the rainfall, the anomalous anticyclone over area 1 changes to the anomalous cyclone. The radiation becomes weaker and the latent heat anomaly turns to be positive, which is a crucial contributor to the decrease of SSTA over area 1.

The right panels in Fig. 12 display a similar evolution for area 2 during JA. From lag = –10 to lag = –2, both net solar radiation and OLR anomalies switch from the maximum to minimum, which corresponds to less radiation and more cloud, accompanied with the northwestward propagation of the anomalous cyclone from the Philippine Sea at the same time (Fig. 12d). Owing to the increase of surface wind anomaly (Fig. 12h), the latent heat anomaly over area 2 changes from relative large negative (lag = –11) to largest positive (lag = –2) (Fig. 12f). This means that the ocean over area 2 releases more latent heat to the atmosphere. The subseasonal sensible heat anomaly is also relatively negligible. In conclusion, before the rainfall events, the northwestward propagation of the anomalous cyclone from the Philippine Sea to South China causes less radiation, more cloud, and more latent heat released to the atmosphere over area 2. Therefore, the ocean over area 2 loses more energy and tends to get colder. After the rainfall, the anomalous cyclone weakens and finally disappears. The ocean over area 2 receives more radiation and releases less latent heat, so the negative SSTA fades and switches to positive anomaly.

4.3 Possible role of the subseasonal SSTA on the circulation

The subseasonal SSTA variation can also have an important influence on the circulation via changing the local thermal gradient (Lau and Nath, 2009), or affecting the lower-level convective instability (Roxy and Tanimoto, 2012; Ren et al., 2013). We hereby discuss the possible role of the subseasonal SSTA on the convective instability. We use the pseudo-equivalent potential temperature (θ_{se}) at 1000 hPa minus that at 850 hPa ($\theta_{se1000} - \theta_{se850}$) to represent the lower-level convective instability. Figure 13 shows the composite subseasonal anomalies of SST, convective instability ($\theta_{se1000} - \theta_{se850}$), θ_{se}, specific humidity and air temperature at 1000 hPa, averaged over area 1 and area 2. Figure 13a shows that the convective instability anomaly over area 1 for MJ group is positive (positive means more unstable) during lag = –4 to lag = 4, which corresponds to the decrease of positive Z850 anomaly during lag = –4 to lag = 4 as shown in Fig. 12a. Figure 13c shows that the anomalies of air temperature and specific humidity at 1000 hPa are at their positive phase from lag = –4 to lag = 4 because of the warm SSTA over area 1 during this period. Therefore, the warm SSTA over area 1 could increase the surface air temperature and humidity, thus affecting the surface θ_{se} and creating unstable conditions. Thus, the positive SSTA in area 1 for MJ group may be favorable for the weakening of the anomalous anticyclone.

For JA group (Fig. 13b), the convective instability anomaly over area 2 is negative (negative means more stable) during lag = –4 to lag = 2, which corresponds to the weakening of negative Z850 as shown in Fig. 12b. Figure 13d shows that the air temperature at 1000 hPa also decreases following the cooling of SST during lag = –4 to lag = 2. However, the humidity is not closely related to the variation of SST in this process. The cold SSTA may just partially modify the convective instability via affecting surface air temperature.

5. Conclusions and discussion

This study addresses the connection between anomalous circulation and SST over the South China–EACR, accompanied with the PHR events over South China during May–August on the subseasonal timescale. The PHR events over South China are categorized into two groups (MJ and JA groups) firstly. By using the criterion that the normalized subseasonal daily rainfall anomalies over South China exceed one standard deviation for at least 3 consecutive days, we selected 63 PHR events during MJ and 59 PHR events

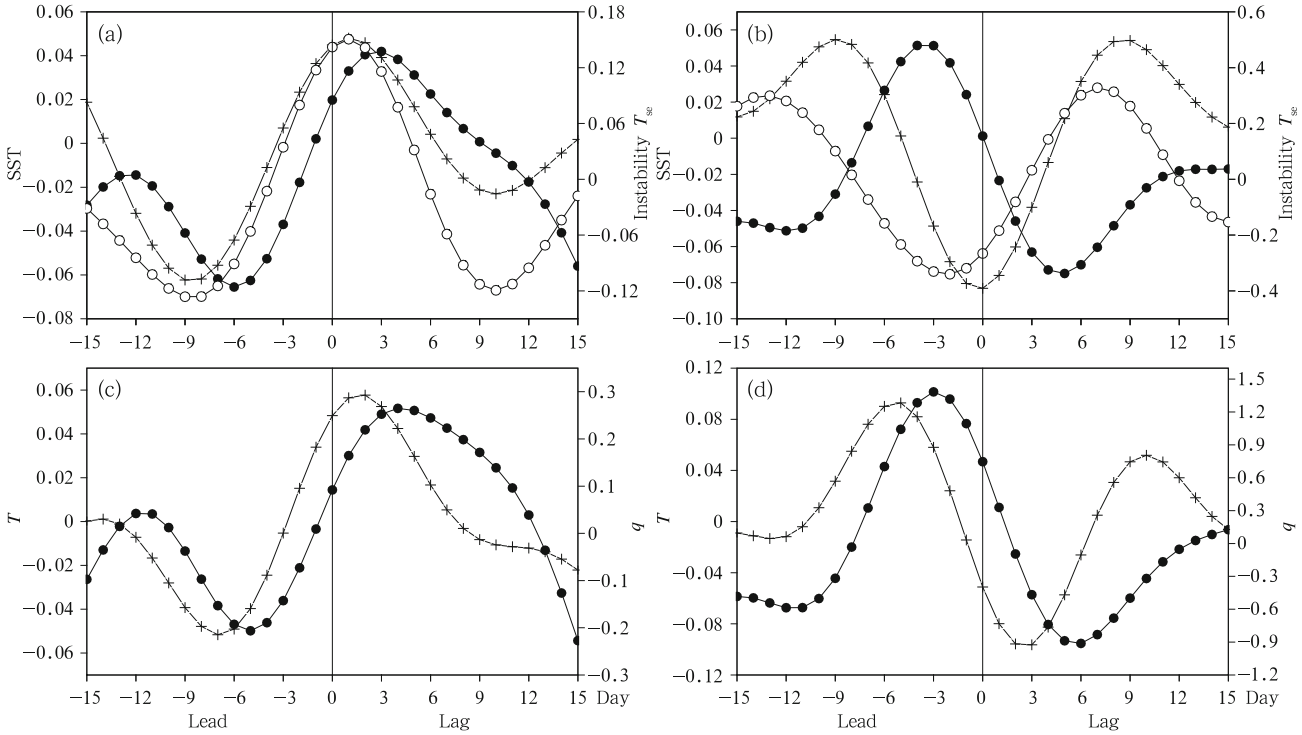

Fig. 13. (a, b) Composite subseasonal anomalies of SST (cross line), convective instability (hollow dot line), θ_{se} (dot line; K) at 1000 hPa, (c, d) specific humidity (dot line; 10^{-4} kg kg^{-1}) and air temperature (cross line; K) at 1000 hPa, averaged over (a, c) area 1 and (b, d) area 2.

during JA over South China. The features and evolution of the circulation anomaly and SSTA over the South China–ECAR on the subseasonal timescale are investigated by performing the lead-lag composite for MJ and JA groups.

For MJ group, the lower-level anomalous circulation pattern during the PHR events exhibits strong convergence over South China, with an anomalous cyclone located over South China and an anomalous anticyclone shaped like a tongue over the SCS. There are three main subseasonal precursor signals at lower levels for MJ group. The first signal is the southward propagation of low-value systems from the mid-high latitude to South China, which is a main contributor to the anomalous cyclone over South China. The second signal is the southeastward propagation of anomalous anticyclone from South China to the SCS, and the third one is the westward propagation of the anomalous anticyclone from the Philippine Sea to the SCS, corresponding to the westward stretch of the WPSH. The latter two signals contribute to the formation of the tongue area during the PHR events. At the upper level, the circulation exhibits an east-west dipole structure, which facilitates a divergence circumstance over South China during the PHR events.

The pattern of lower-level circulation anomaly in JA is similar to that in MJ over the South China–EACR, but the feature of the propagation is different. The anomalous cyclone over South China during JA PHR events originates from the weak anomalous cyclone over the Philippine Sea several days before the rainfall. This weak anomalous cyclone propagates northwestward to South China and gets strengthened gradually. The westward extension of the WPSH is also prominent for JA group, which is a dominant factor to the formation of the tongue area in JA. The upper-level anomalous circulation pattern for JA group with a northeast-southwest dipole structure is also constructive for the anomalous divergence at upper level over South China. The different mean states

of the WPSH between MJ and JA may be an important reason for the subseasonal circulation differences between the two groups of PHR events. On the aspect of the water vapor transport accompanied with the two groups of PHR events, the westward stretch of the WPSH before the rainfall is in favor of the westward transport of water vapor from the western Pacific to South China.

On the oceanic aspect, for MJ group, positive SSTA lies over the SCS and the Philippine Sea while negative SSTA exists along the East Asian coastal line. The co-variation of subseasonal anomalies of SST and Z850 over the SCS and the Philippine Sea indicates a phase difference between the circulation anomaly and SSTA on the subseasonal timescale during the MJ PHR events. Before the rainfall, the anomalous anticyclone over the SCS and the Philippine Sea is intensified due to westward propagation of the WPSH and southeastward propagation of the anomalous anticyclone from South China. Meanwhile, the local ocean receives more radiation under the weak-convection and less-cloud condition. The negative latent heat anomaly indicates that the ocean loses less energy. Therefore, the ocean over the SCS and the Philippine Sea is in favor of getting warmer. For JA group, robust negative SSTA occupies the South China coastal region. The local Z850 anomaly also leads the SSTA for several days. The cold SSTA over the South China coastal region is driven by the local anomalous cyclone. Before the rainfall, the anomalous cyclone over the South China coastal region strengthens because of the northwestward propagation of the anomalous cyclone from the Philippine Sea. Thus, the local ocean receives less radiation under the strong-convection and more-cloud condition. The latent heat anomaly over the area is positive, leading to more energy release over the local ocean. The above factors are favorable for the decrease of SSTA over the South China coastal region.

In general, the SSTAs over the key oceanic region for MJ and JA groups are mainly driven by the circulation anomaly via processes of radiation and latent heat fluxes. The SSTAs also affect the circulation via changing lower-level convective instability. For MJ group, the warm SSTA during the PHR events could increase the surface air temperature and humidity, thus creating the local unstable condition. For JA group, the negative SSTA may partially modify the convective instability via affecting surface temperature.

In this study, we have focused on the circulation anomaly and SSTA accompanied with PHR events on the subseasonal timescale. The differences between the PHR events on the subseasonal timescale and precipitation on interannual, interdecadal, and synoptic timescales over South China also need attention. On interannual and interdecadal timescales, the SSTAs in the central-eastern Pacific (El Niño/La Niña), the western Pacific warm pool, and the Bay of Bengal, can usually be a precursor signal for the circulation and rainfall anomalies over East Asia (Huang and Wu, 1989; Liang and Wu, 2001; Chan and Zhou, 2005; Zhou et al., 2009). The subseasonal SSTA variations are forced by the subseasonal circulation anomalies via heat fluxes based on some observations (Wu, 2010; Roxy and Tanimoto, 2012; Ren et al., 2013). This is supported by our results as shown in Fig. 12. For precipitation on the synoptic timescale, studies are mainly about the mesoscale structure and weather pattern during a rainfall process (Sun et al., 2002; Zhang and Ni, 2009). Therefore, the PHR defined in this paper has unique features in terms of the air-sea relationship, compared with precipitation on interannual, interdecadal, and synoptic timescales.

REFERENCES

Bao Ming, 2007: Statistical analysis of the persistent heavy rains in the last 50 years over China and their associated large-scale circulation. *Chinese J. Atmos. Sci.*, **31**(5), 779–792. (in Chinese)

Cao Xin, Ren Xuejuan, Yang Xiuqun, et al., 2012: The quasi-biweekly oscillation characteristics of persistent severe rains and associated circulation anomaly over Southeast China from May to August. *Acta Meteor. Sinica*, **70**(4), 766–778. (in Chinese)

——, ——, and Sun Xuguang, 2013: Low-frequency oscillations of persistent heavy rainfall over the Yangtze-Huaihe River basin. *Journal of the Meteorological*

Sciences, doi: 10.3969/2012jms.0165. (in Chinese)

Chan, J. C. L., and W. Zhou, 2005: PDO, ENSO and the early summer monsoon rainfall over South China. *Geophys. Res. Lett.*, **32**, L08810, doi: 10.1029/2004GL022015.

Chen, Y., and P. M. Zhai, 2013: Persistent extreme precipitation events in China during 1951–2010. *Clim. Res.*, **57**, 143–155, doi: 10.3354/cr01171.

Ding Yihui, et al., 1993: *Study on the 1991 Excessively Heavy Rain over Yangtze-Huaihe River Basin*. China Meteorological Press, Beijing, 255 pp. (in Chinese)

——, and J. C. L. Chan, 2005: The East Asian summer monsoon: An overview. *Meteor. Atmos. Phys.*, **89**, 117–142.

Ding Zhiying, Liu Caihong, Chang Yue, et al., 2010: Study of double rain bands in a persistent rainstorm over South China. *J. Trop. Meteor.*, **16**(4), 380–389.

Hu Liang, He Jinhai, and Gao Shouting, 2007: An analysis of large-scale conditions for persistent heavy rainfall in South China. *J. Nanjing Inst. Meteor.*, **30**(3), 345–351. (in Chinese)

Huang Ronghui and Wu Yifang, 1989: The influence of ENSO on the summer climate change in China and its mechanism. *Adv. Atmos. Sci.*, **6**(1), 21–32.

Jiang Zhihong, Liang Zhuoran, Liu Zhengyu, et al., 2011: A diagnostic study of water vapor transport and budget during heavy precipitation over the Huaihe River basin in 2007. *Chinese J. Atmos. Sci.*, **35**(2), 361–372. (in Chinese)

Kanamitsu, M., W. Ebisuzaki, J. Woollen, et al., 2002: NCEP-DOE AMIP-II reanalysis (R-2). *Bull. Amer. Meteor. Soc.*, **83**, 1631–1643.

Lau, N. -C., and M. J. Nath, 2009: A model investigation of the role of air-sea interaction in the climatological evolution and ENSO-related variability of the summer monsoon over the South China Sea and western North Pacific. *J. Climate*, **22**, 4771–4792.

Li Jianping and Zhu Jianlei, 2010: Climatological features of the western Pacific subtropical high southward retreat process in late spring and early summer. *Acta Meteor. Sinica*, **24**(4), 397–412.

Liang Jianyin and Wu Shangsen, 2001: Formation reasons of drought and flood in the rainy season of Guangdong and the preceding impact factors. *J. Trop. Meteor.*, **17**(2), 97–108. (in Chinese)

Liebmann, B., and C. A. Smith, 1996: Description of a complete (interpolated) outgoing longwave radiation dataset. *Bull. Amer. Meteor. Soc.*, **77**, 1275–1277.

Lu Er and Ding Yihui, 1997: Low frequency oscillation in East Asia during the 1991 excessively heavy rain over the Yangtze-Huaihe River basin. *Acta Meteor. Sinica*, **11**(1), 12–22.

Lu, R. Y., and B. W. Dong, 2001: Westward extension of North Pacific subtropical high in summer. *J. Meteor. Soc. Japan*, **79**(6), 1229–1241.

Mao Jiangyu and Wu Guoxiong, 2005: Intraseasonal variability in the Yangtze-Huaihe River rainfall and subtropical high during the 1991 Meiyu period. *Acta Meteor. Sinica*, **63**(5), 762–770. (in Chinese)

Niu Ruoyun, Zhang Zhigang, and Jin Ronghua, 2012: The atmospheric circulation features of two persistent heavy rainfalls over southern China in the summer of 2010. *J. Appl. Meteor. Sci.*, **23**(4), 385–394. (in Chinese)

Pan, W. J., J. Y. Mao, and G. X. Wu, 2013: Characteristics and mechanism of the 10–20-day oscillation of spring rainfall over southern China. *J. Climate*, **26**, 5072–5087, doi: 10.1175/JCLI-D-12-00618.1.

Qian Yongfu, Zhang Qiong, and Zhang Xuehong, 2002: The South Asian high and its effects on China's mid-summer climate abnormality. *J. Nanjing Univ.*, **38**(3), 296–307. (in Chinese)

Qiang Xuemin and Yang Xiuqun, 2008: Onset and end of the first rainy season in South China. *Chinese J. Geophys.*, **51**(5), 1333–1345. (in Chinese)

Ren Xuejuan, Yang Xiuqun, and Sun Xuguang, 2013: Zonal oscillation of the western Pacific subtropical high and subseasonal SST variations during the Yangtze River persistent heavy rainfall events. *J. Climate*, doi: 10.1175/JCLI-D-12-00861.1.

Roxy, M., and Y. Tanimoto, 2012: Influence of sea surface temperature on the intraseasonal variability of the South China Sea summer monsoon. *Climate Dyn.*, **39**, 1209–1218.

Shi Xueli and Ding Yihui, 2000: A study on extensive heavy rain processes in South China and the summer monsoon activity in 1994. *Acta Meteor. Sinica*, **58**(6), 666–678. (in Chinese)

Sun Jian, Zhao Ping, and Zhou Xiuji, 2002: The mesoscale structure of a South China rainstorm and the influence of complex topography. *Acta Meteor. Sinica*, **60**(3), 333–346. (in Chinese)

Tang Yanbing, Gan Jingjing, Zhao Lu, et al., 2006: On the climatology of persistent heavy rainfall events in China. *Adv. Atmos. Sci.*, **23**(5), 678–692.

Tao Shiyan and Chen Longxun, 1987: A review of recent research on the East Asian summer monsoon in China. *Monsoon Meteorology*. Chang C. P., and T. N. Krishnamurti, Eds., Oxford University Press, New York, 60–92.

Vecchi, G. A., and D. E. Harrison, 2002: Monsoon breaks and subseasonal sea surface temperature variability in the Bay of Bengal. *J. Climate*, **15**, 1485–1493.

Wang, B., J. Liu, J. Yang, et al., 2009: Distinct principal modes of early and late summer rainfall anomalies in East Asia. *J. Climate*, **22**, 3864–3875.

Wang Lijuan, Guan Zhaoyong, and He Jinhai, 2007: Features of large-scale circulation for the flash-flood-producing rainstorm over South China in June 2005 and its possible cause. *J. Nanjing Inst. Meteor.*, **30**(2), 145–152. (in Chinese)

——, Chen Xuan, Guan Zhaoyong, et al., 2009: Features of the short-term position variation of the western Pacific subtropical high during the torrential rain causing severe floods in southern China and its possible cause. *Chinese J. Atmos. Sci.*, **33**(5), 1047–1057. (in Chinese)

Wang, L., T. Li, and T. J. Zhou, 2012: Intraseasonal SST variability and air-sea interaction over the Kuroshio extension region during boreal summer. *J. Climate*, **25**, 1619–1634.

Wang Zunya and Ding Yihui, 2008: Climatic characteristics of rainy seasons in China. *Chinese J. Atmos. Sci.*, **32**(1), 1–13. (in Chinese)

Wu, R. G., 2010: Subseasonal variability during the South China Sea summer monsoon onset. *Climate Dyn.*, **34**, 629–642.

——, B. P. Kirtman, and K. Pegion, 2008: Local rainfall-SST relationship on subseasonal timescales in satellite observations and CFS. *Geophys. Res. Lett.*, **35**, L22706, doi: 10.1029/2008GL035883.

Wu Zhiwei, Jiang Zhihong, and He Jinhai, 2006: Comparison analysis of flood and drought features among the first flood period in South China, Meiyu period in the Yangtze River and the Huaihe River valleys, and the rainy season in North China in the last 50 years. *Chinese J. Atmos. Sci.*, **30**(3), 391–401. (in Chinese)

Yang, J., B. Wang, B. Wang, et al., 2010: Biweekly and 21–30-day variations of the subtropical summer monsoon rainfall over the lower reaches of the Yangtze River basin. *J. Climate*, **23**, 1146–1159.

——, Q. Bao, B. Wang, et al., 2013: Distinct quasi-biweekly features of the subtropical East Asian monsoon during early and late summers. *Climate Dyn.*, doi: 10.1007/s00382-013-1728-6.

Yin Zhicong, Wang Yafei, and Yuan Dongmin, 2011: Analysis of the interannual variability of the Meiyu quasi-biweekly oscillation and its previous strong influence signal. *Trans. Atmos. Sci.*, **34**(3), 297–304. (in Chinese)

Zhang Xiaohui and Ni Yunqi, 2010: A diagnostic case study on the comparison between the frontal and non-frontal convective systems. *Acta Meteor. Sinica*, **24**(1), 66–77.

Zhou, T. J., R. C. Yu, J. Zhang, et al., 2009: Why the western Pacific subtropical high has extended westward since the late 1970s. *J. Climate*, **22**, 2199–2215.